

Duquesne University

## Duquesne Scholarship Collection

---

Electronic Theses and Dissertations

---

Fall 12-17-2021

# DETECTING VIRAL PARTICLES IN VITRO USING PHOTOACOUSTIC FLOW CYTOMETRY

Anie-Pier Samson

Follow this and additional works at: <https://dsc.duq.edu/etd>



Part of the [Biomedical Devices and Instrumentation Commons](#), and the [Other Biomedical Engineering and Bioengineering Commons](#)

---

### Recommended Citation

Samson, A. (2021). DETECTING VIRAL PARTICLES IN VITRO USING PHOTOACOUSTIC FLOW CYTOMETRY (Master's thesis, Duquesne University). Retrieved from <https://dsc.duq.edu/etd/2048>

This Immediate Access is brought to you for free and open access by Duquesne Scholarship Collection. It has been accepted for inclusion in Electronic Theses and Dissertations by an authorized administrator of Duquesne Scholarship Collection.

DETECTING VIRAL PARTICLES IN VITRO USING PHOTOACOUSTIC FLOW  
CYTOMETRY

A Thesis

Submitted to the Rangos School of Health Sciences

Duquesne University

In partial fulfillment of the requirements for  
for the degree of Master of Science

By

Anie-Pier Samson

December 2021

Copyright by  
Anie-Pier Samson

2021

DETECTING VIRAL PARTICLES IN VITRO USING PHOTOACOUSTIC FLOW  
CYTOMETRY

By

Anie-Pier Samson

Approved November 10, 2021

---

Dr. John Viator  
Chair, Department of Engineering  
(Committee Chair)

---

Dr. Bin Yang  
Professor of Engineering  
(Committee Member/Reader)

---

Dr. Kristen Butela  
Professor of Biological Sciences  
(Committee Member/Reader)

## ABSTRACT

### DETECTING VIRAL PARTICLES IN VITRO USING PHOTOACOUSTIC FLOW CYTOMETRY

By

Anie-Pier Samson

December 2021

Thesis supervised by Dr. John Viator

The Covid-19 pandemic is a powerful example of just how damaging the rapid spread of an unknown virus can be. Viruses have the ability to spread rapidly amongst individuals if not treated and controlled. The first key step towards treatment is the timely and specific diagnosis of the virus causing the infection. An innovative method for the rapid detection of viral particles in solution consists of tagging the viral particles paired with using photoacoustic flow cytometry to irradiate the particles and get a signal. The high affinity of Streptavidin for Biotin can be used to bind Streptavidin-coated microspheres to biotinylated antibodies. Monoclonal antibodies will be

used to make sure that each one of them can only attach to one antigen on each viral particle. Using microspheres allows for a close approximation of the number of microspheres that can bind to each viral particle at a rate of approximately 6 microspheres per virion. However, the margin of error is thought to be high, due to the small difference between the detection signal threshold between one single particle and six of them bound together. The solution to eliminate this error resides in a multi-step process resulting in engineered microsphere complexes that can be detected by the system. Increasing the microsphere complex size by at least 3 orders of magnitude allows us to maintain the detection signal threshold to detect the particles at the standard threshold. Using photoacoustic flow cytometry to detect viral particles was never attempted before and would expand the range of applications for this system.

## Table of Contents

LIST OF FIGURES.....	vii
LIST OF TABLES .....	viii
CHAPTER 1: INTRODUCTION.....	1
1.1 PHOTOACOUSTIC FLOW CYTOMETRY .....	2
1.2 ANALYTE DISTINCTION.....	4
1.3 DETECTION OF VIRAL PARTICLES.....	5
CHAPTER 2: MATERIALS AND METHODS .....	10
2.1 DETERMINATION OF PROTEIN CONCENTRATION.....	14
2.2 PREPARATION OF MICROSPHERES .....	15
2.3 BIOTINYLATED SP1 AND TYPE 5 ANTIBODIES .....	15
2.4 BIOTINYLATED TYPE 5 HEXON PROTEIN.....	16
2.5 ATTACHING BIOTINYLATED ANTIBODIES TO PREPARED MICROSPHERES...	16
2.6 LABELLING SV40 .....	17
2.7 FORMATION OF MICROSPHERE COMPLEXES .....	17
CHAPTER 3: RESULTS.....	18
3.1 NEGATIVE CONTROLS.....	18
3.2 POSITIVE CONTROLS .....	19
3.3 EXPERIMENTAL DATA .....	20
CHAPTER 4: DISCUSSION.....	22
4.1 FUTURE DIRECTIONS.....	24
4.2 CONCLUSION .....	25
REFERENCES .....	26

## LIST OF FIGURES

Figure 1: Schematics of the photoacoustic flow cytometry system.....	4
Figure 2: Schematics of labeled photoacoustic flow chamber.....	5
Figure 3: Representation of MC1 .....	6
Figure 4: Size representation of the diameter of the two microsphere complexes .....	9
Figure 5: Light microscope pictures of CV-1 cells (LEFT) and SV40 (RIGHT). These two pictures show the cytopathic effect. The cells on the right have been lysed and SV40 has reproduced.....	13
Figure 6: Illustration of the process of attaching biotinylated antibodies to microspheres from Bangs Laboratories. The illustrated oligonucleotide represents the antibody or antigen used in this procedure.....	17



## LIST OF TABLES

Table 1: Absorbance and calculated protein concentration for each of the antibodies and antigen used. ....	14
Table 2: Negative controls showing that no analyte contained in the microsphere complexes contain photo absorbing matter.....	19
Table 3: Positive controls showing that 0.19 $\mu$ m microspheres cannot absorb laser light until present in a concentration of $10^8$ microspheres/ml. 1 $\mu$ m microspheres absorb laser light much better and can be detected starting from a $10^5$ microspheres/ml concentration.....	20
Table 4: Experimental data showing that ratios of SV40 to VP1 antibody Microspheres to Type 5 hexon protein microspheres. Increasing the amount of Type 5 hexon protein microspheres does not alter the outcome much because the surface area of the first microsphere.....	21
Table 5: Summary of the experimental data. The number of detections obtained from the second Microsphere Complexes is two orders of magnitude higher than that of the first Microsphere Complexes.....	21

## CHAPTER 1: INTRODUCTION

Globalization only means viral infection when devastating consequences are involved. Viral infections are among the top cause of mortality worldwide, and with accessibility to new environments being so open, viruses have a greater chance to spread among and infect populations [1]. With this global burden becoming an increasing threat, as it was experienced with the coronavirus 2019 outbreak, there is a need for methods that can provide rapid and cost-effective diagnostics. By detecting and accurately identifying the virus responsible for an infection, controlling the spread of the infection becomes easier and requires less resources.

Viral particle detection is generally done by identifying viral particles, RNA or DNA, antigens, or specific antibodies [2]. Currently, viral particles assays are done using mainly solid-phase immunoassays, cell culture, polymerase chain reaction (PCR), antibody agglutination, and antigen testing. The current benchmark for viral particle identification is PCR which allows for semi quantitative precise quantification of the number of viral particles in a clinical sample. It also has the ability to identify viral oligonucleotides, a piece of information crucial to reflect viral replication and the active infection rate. However, this method is very timely as it takes days to develop a sample to the point where it is ready to be processed. PCR also often happens to be affected by multiple factors like the salinity of the environment, the concentration of particles, and other inhibitors. The high-cost and need for trained personnel would also be cons of using PCR if a better method came along. Another method of viral detection is solid-phase immunoassays (SPIs). This method can detect viral antigens in a sample rapidly and reliably. It works by immobilizing antibodies to a reliable support. Viral antigens will then bind to the specifically selected antibodies and effectively assess the number of viral particles of that type

present in solution. The high specificity of this technique renders it very attractive for researchers. However, this process is so simplified that it is not as reliable as PCR and is timely. The problems with antibody agglutination and antigen testing are that they both require a large concentration of viral particles to be accurate and they both are not quantitative. All combined, these methods still cannot detect close to a third of the respiratory viral infections, viral gastroenteritis, and viral encephalitis [3]. Therefore, it is clear that the viral particle detection area can use a more rapid, efficient, specific, and cost-effective way to analyze a viral sample. A fully comprehensive diagnosis that can be combined with point-of-care applications would have a significant impact on controlling the spread of viral infections at the source. Infected individuals can be rapidly isolated and treated appropriately, minimizing the collateral medical and emotional costs. The need for a better way to readily quantify the number of viral particles in a complex sample can be met by the introduction photoacoustic flow cytometry in the vast world of *in vitro* viral assays.

## **1.1 PHOTOACOUSTIC FLOW CYTOMETRY**

Photoacoustic flow cytometry (PAFC) uses the photoacoustic effect to detect the desired analytes in a sample. The photoacoustic effect can be described as the induction of sound waves produced from an optical source also referred to as laser-induced ultrasound. The two base components of any photoacoustic system are the pulsed laser and transducer. Lasers are able to deliver precise wavelengths and energy to a sample in defined amounts of time. Transducers are commonly used in many industrial applications from depth profiling to prenatal ultrasound machines. The photoacoustic flow cytometry set up is illustrated in figure 1. In Photoacoustics, the absorption of laser energy causes a rapid heating and cooling of an object resulting in

thermoplastic expansion and contraction. This expansion and contraction phenomenon is characterized by a condition known as stress confinement. Stress confinement of an object is determined by the physical properties of each cell and the time frame that laser energy is deposited. When an object is under stress confinement it will expand and contract creating pressure waves that can be detected [4]. Photoacoustic flow cytometry takes advantage of these characteristics for detection of objects under flow. The flow chamber in which this process takes place can be seen in figure 2.

PAFC has been a great contender in the diagnostics world for many years. Shashkov et al. demonstrated the ability to detect particles under flow *in vivo* by labeling the particles of interest with carbon nanotubes or gold nanorods [5]. The extensive work of Edgar et al. with PAFC detected circulating tumor cells in a blood sample by using the intrinsic melanin in the cells as photo absorber. Edgar et al. also demonstrated the ability to detect bacteria *in vitro* by tagging bacterial cells with bacteriophage. This technology has the ability to detect rare particles in solutions by making use of the photoacoustic effect [6] The key element into detecting any particles with this system is the photo absorbing element. If the particle of interest does not inherently contain a sufficient amount of photo absorbing matter, it needs to be tagged with a light absorbing element. PAFC has already been used to detect melanoma and bacterial cells in complex environments [6, 7]. The next logical step is to use the versatility of the system to detect viral particles in a more timely and accurate fashion than the current detection methods can. Virions, unlike circulating tumor cells (CTC's) or bacterial cells, lack some essential components to be easily detected. Accordingly, special tagging complexes were engineered to allow the PAFC system to detect undetectable viral particles.

## 1.2 ANALYTE DISTINCTION

The difference in size between all three categories of particles also greatly affects detection. The average diameter of a melanoma cell is  $18\mu\text{m}$  and the average diameter of a bacterial cell ranges from  $0.5$  to  $5\mu\text{m}$ . However, the average diameter of a viral particle ranges from  $20$ - $500$  nm. The multiple orders of magnitude difference between the three categories mean that an alternate method of detection must be used to detect viral particles. The detection of melanoma cells can be achieved because of the intrinsic melanin found in the cells which acts as a photo absorber. Bacterial cells, having intrinsically no photo absorbing component, can be detected by using tagged bacteriophage as photo absorbers. Viral particles lack an intrinsic photo-absorbing component. Tagging the viral particles with naturally-occurring tags of adequate size presents a difficulty due to their small size. Using this tagging technique, specifically designed and manufactured photo-absorbing tags have been developed for virion detection using the PAFC system.

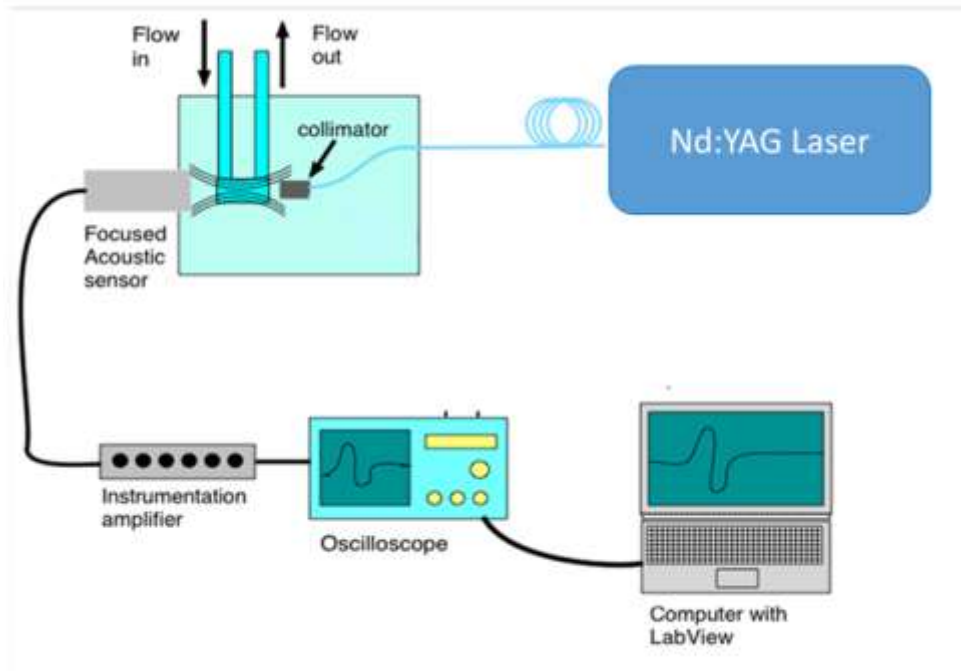
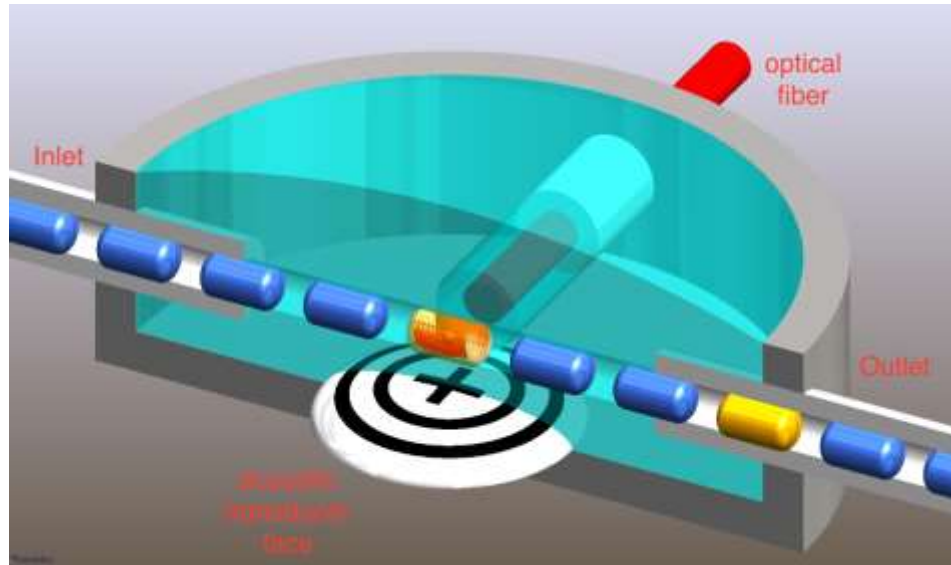


Figure 1: Schematics of the photoacoustic flow cytometry system



*Figure 2: Schematics of labeled photoacoustic flow chamber*

### 1.3 DETECTION OF VIRAL PARTICLES

Simian Virus 40 is one of the best known and studied viruses in the world. It was originally discovered as a contaminate of the Salk Polio vaccine and quickly became a model virus of Virology and host interactions [8]. Polyomaviruses such as Simian Virus 40 (SV40) are known to be of the simplest viruses with double-stranded DNA genomes. Because of its simplicity and widely understood mechanisms, the SV40 system has been used to study a wide range of processes within the immunology and molecular biology worlds [9]. SV40 was chosen as the viral model for this assay because of its simple icosahedral structure and the vast amount of knowledge collected over the years on its mechanisms. Icosahedral symmetry plays an important role in the study of viral capsid proteins, eventually leading to more knowledge on the viral structure made out of asymmetric blocks [10].

SV40 virion particle self-assemble from a single repeating subunit called VP1. The capsid is built from 72 pentamers, each contains five VP1 subunits, for a total of 360 VP1 identical subunits in the mature capsid [11]. For this reason, any tag or antibody that attaches to the VP1 subunit of SV40 will have multiple binding positions equally distributed on the exterior of the virion particle. Antibodies to VP1 have been attached to photo-absorbing microspheres and these antibody-covered microspheres can attach to the capsid of SV40. This yields a bundle of microspheres that are bound to individual viral particles. SV40 has a diameter of 45nm while a microsphere has a diameter of 0.19 $\mu$ m. The size difference between one microsphere and one viral particle allows for one microsphere to bind to each side of the viral particle. Thus, one virion becomes surrounded by six microspheres, creating the first microsphere complex (MC1).

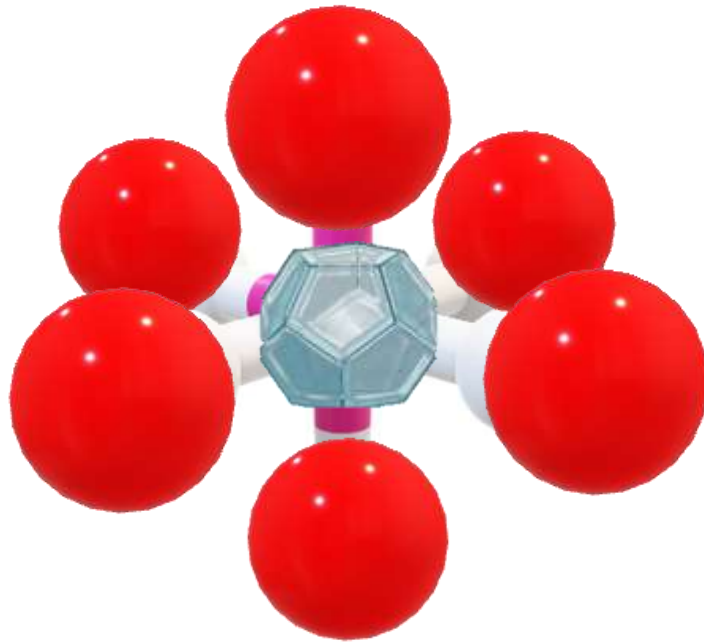


*Figure 3: Representation of MC1*

The diameter of the detectable unit then increases from 45nm to 0.425 microns. However, even though the microsphere complex gives a tenfold increase from the initial undetectable size of a single virion, it gives rise to a new problem. The difference in diameter between a single free-floating microsphere and that of a microsphere complex is only 0.235micron. The size of the difference between the two analytes is not big enough for the PAFC system to be able to distinguish them from each other. As comparison, in the bacterial detection model, the difference in size between a single tagged phage (~0.1 $\mu$ m) and a tagged bacterial cell (~1 $\mu$ m) is at least a tenfold increase. Bacterial detection is achieved by using units that are much smaller than the desired analytes. This technique uses the same concept, but binds significantly bigger units to the desired analytes. Although these two techniques seem very similar, one problem arises from the difference in size between virions and microspheres. How to determine between a detection obtained from a single free-floating microsphere and one obtained from a microsphere complex?

To alleviate this problem, the microspheres that are added first and bound to the viral particles are covered in VP1, an antibody to SV40. Another antibody, which binds to a different receptor protein than that of SV40 is also tethered to the microspheres constituting this first layer. The second antibody/antigen pair consists of an adenovirus, Adenovirus Type 5 hexon protein and an anti-adenovirus type 5 antibody. The second antigen is biotinylated to a second sample of microspheres. After attaching the first layer of microspheres to the viral particles, a second layer of microspheres is added. This time, those microspheres are coated in a different receptor protein and will bind to the other antibodies present on the first layer of microspheres.

Adenovirus vectors have also been extensively studied and are well-understood. Choosing another type of virus that uses a different attachment protein than that of SV40 is crucial for the success of this study. Using two completely different antigen/antibody reactions



ensures the specificity of binding as well as eliminating the need of removing unbound microspheres. For this study, the ADV type 3 antigen was chosen to be targeted by an anti-adenovirus antibody. ADV type 3 is a naturally occurring antigen that is very stable and commercially available.

The icosahedral structure of SV40 and the tenfold difference between the size of a microsphere and the size of a virion mean that only one microsphere will be able to bind to each side of the viral particle. By dissecting the MC1, one can observe that the diameter contains two microspheres and one virion. The microspheres have a nominal diameter of  $0.19\mu\text{m}$  and the virion has a diameter of  $0.045\mu\text{m}$ . The total diameter of MC1 adds up to be  $0.425\mu\text{m}$ , yielding a radius of  $0.2125\mu\text{m}$ . The total volume of the microsphere complexes can be modeled as that of a sphere. Thus, the volume of MC1 is:

$$\frac{4}{3}\pi(0.2125)^3 = 0.0402\mu\text{m}^3$$

By adding another layer of microspheres to the MC1's, the new diameter of the new microsphere complexes (MC2) is now  $0.850\mu\text{m}$ . The volume of MC2 is therefore given by:

$$\frac{4}{3}\pi(0.425)^3 = 0.322\mu\text{m}^3$$

Due to the volume of the microsphere complex resembles that of a sphere, doubling the radius means that the volume is exactly 8 times greater after doubling the size of the microsphere complex, thus the main focus of increasing the radius of the complex. In this volume range, the photoacoustic flow system has already been proven to be able to detect tagged bacterial cells of this size. Using anterior research and results, detecting viral particles can be achieved using microsphere complexes because of their comparable size to a tagged bacterial cell. The size comparison of the two microsphere complexes is illustrated in figure 4.

Using this technique of building a microsphere complex consisting of two layers of 0.19  $\mu\text{m}$  microspheres we are able to reliably detect signal viral particles without detecting single free floating unbound microspheres. This method allows us to isolate and quantify viral particles in a sample. Isolation of single viral particles can be very beneficial in studying heterogeneity in virion population [12]. Additionally, single read sequencing technologies have now made single particle research more practical and attainable to answer scientific questions previously unattainable [13].

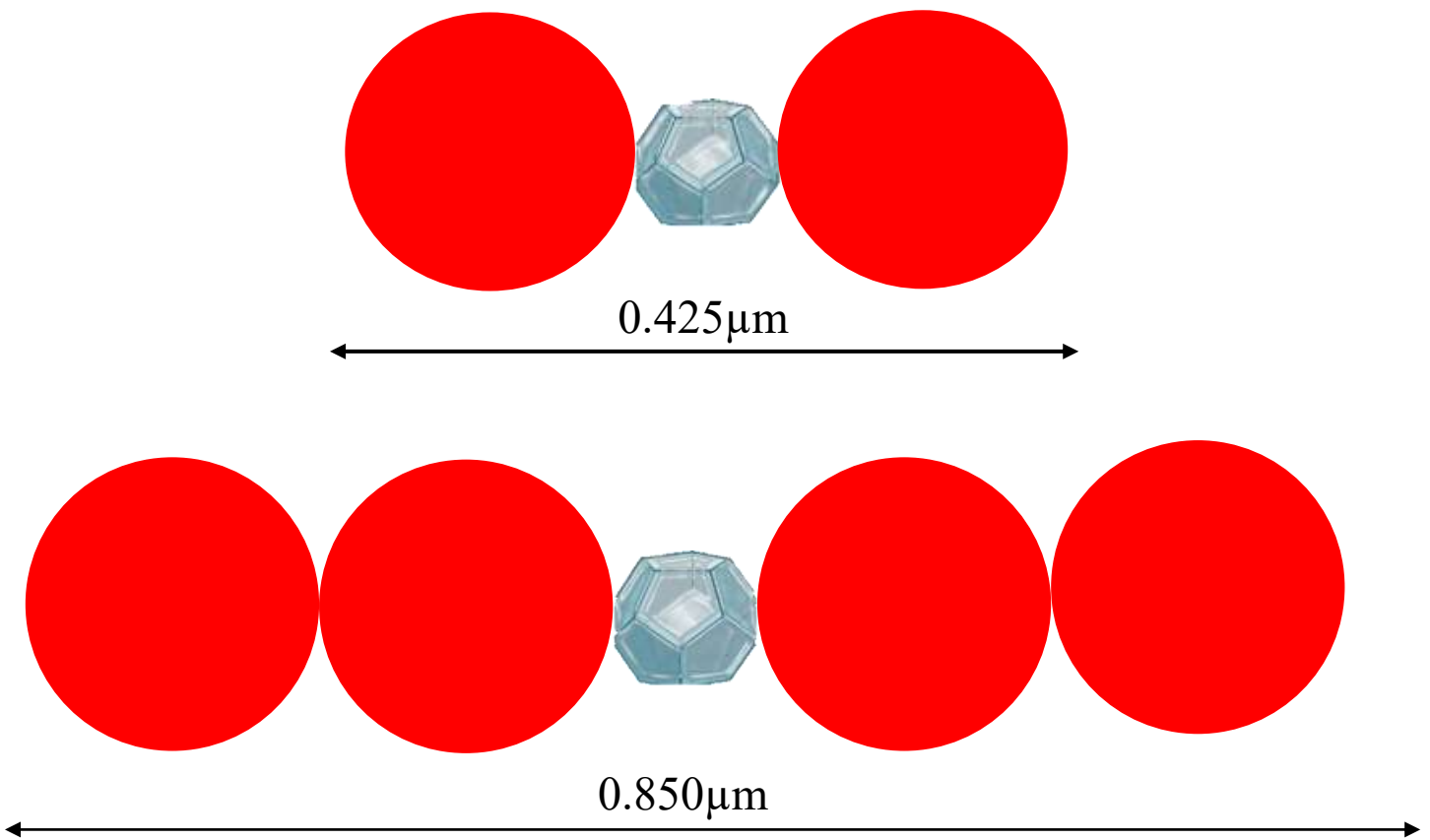


*Figure 4: Size representation of the diameter of the two microsphere complexes*

## CHAPTER 2: MATERIALS AND METHODS

CV-1 cells were used as the host cells for SV-40 replication. The growth media necessary for optimal growth of CV-1 cells (ATCC CCL-70) is made by combining fetal bovine serum (FBS) (ATCC 30-2020), pen/strep solution (ATCC 30-2300) and Eagle Minimum Essential Medium (ATCC 30-2003). FBS and the pen/strep solution are thawed in a water bath (37°C) until completely thawed through. To obtain a concentration of 10% FBS in the growth medium, add 50ml of FBS to a new 500ml bottle of EMEM. In order to eliminate the possibility of bacterial contamination, 5ml of pen-strep solution were added to the growth medium to obtain a concentration of 1%. Media was mixed thoroughly by agitating the mixture until all the components are well combined. Containers were labeled and stored between 2 and 8°C.

Aseptic technique was used when handling all media and cell lines. The Biohood is sanitized with 70% ethanol solution and sterilized under the UV light for five minutes with every use. Gloves are worn at all times and sterilized each time during the handling of cells to prevent cell contamination. Aseptic technique was carried throughout all procedures as well as performed in a biohood. Once the work surface is ready, the blower is turned on to eliminate the possibility of outside contamination and to keep a sterile field. Two 15ml falcon tubes and a falcon tube rack are sprayed with 70% ethanol and placed in the biohood. The assembled growth medium, a 10ml serological pipette, and an automatic pipette are also disinfected and placed in the biohood. Each item was carefully wiped down inside the biohood. Next, the dry-ice frozen vial of CV-1 cells was thawed in a water bath at 37°C. Once the content of the vial was completely thawed, the vessel was sprayed and wiped down in the biohood. The cells were added to a 15ml falcon tube followed by 10ml of growth medium. The lid was placed on the tube before the tube was centrifuged at 1600rpm for 10 minutes at 24°C. While the cells were being

centrifuged, a T-25 cell-culture flask was sterilized, labelled, and added to the biohood. After centrifugation was completed, the falcon tube containing the cells was taken out of the centrifuge, sterilized once again, and wiped down in the biohood. The cells formed a pellet at the bottom of the tube. This allowed for the medium to be slowly aspirated in the second falcon tube to leave the pellet undisturbed. 3ml of growth medium was added to the pelleted cells. The cells were resuspended using a vortex and then added to the culture flask. The flask was carefully sprayed down with 70% ethanol and placed in the CO<sub>2</sub> incubator at 36.5°C.

The growth medium was changed every 72 hours. Between changes, the cells were observed under a light microscope (Leica DMI4000B). After the sanitation of the Biohood with 70% ethanol solution and decontaminated under the UV light for five minutes, the blower was turned on. The cell flask was carefully sprayed with 70% ethanol solution and wiped off in the Biohood. The growth medium, two 15ml falcon tubes, a falcon tube rack, a 10 ml serological pipette, and an automatic pipette were sterilized and placed in the biohood before getting wiped down. The cells were added to a 15ml falcon tube. The lid was placed on the tube before the tube was centrifuged at 1600rpm for 10 minutes at 24°C. The centrifuged tube was sprayed with 70% ethanol solution before entering the Biohood and getting wiped down. The old medium was discarded in the second falcon tube. 3ml of new growth medium was added to the pelleted cells using the automatic pipet. The cells were resuspended using the vortex and poured back into the same flask. The flask was carefully sprayed down with 70% ethanol and placed in the CO<sub>2</sub> incubator at 36.5°C.

Once the cells reached confluence, subculturing was performed. Following aseptic technique, the culture medium was removed from the culture flask. The cell layer was rinsed with 0.25% (w/v) Trypsin-0.53mM EDTA to remove all serum that contains trypsin inhibitor.

The flask was put under the microscope and 3ml of Trypsin-EDTA solution was added to the flask. It is very important to not move the flask after adding the Trypsin-EDTA solution to the flask to avoid the agglutination of cells. The cells were constantly monitored and observed under the microscope to know when the extracellular matrix has dissolved and the cells are released. Once complete dispersion was achieved, 6ml of growth medium was added to the flask. The content of the flask was poured into a 15ml Falcon tube and centrifuge at 1600RPM for 10 minutes. The media on top of the pelleted cells was aspirated and 6 ml of new growth medium was added to the tube. The cells were resuspended using a vortex and split evenly between two new culture flasks. The flasks were labelled and place into the CO<sub>2</sub> incubator. This process was repeated once more when both flasks were confluent.

Once the CV-1 cells in the four flasks reached 80-90% confluence, SV40, also known as Macaca mulatta polyomavirus 1 (ATCC® VR-1901™), was added to one of the flasks. The SV40 aliquot was thawed in a water bath. The cells were inoculated with 1ml of SV40 to reach an optimal MOI of 0.01. The flask was placed in the humidified 5% CO<sub>2</sub> incubator for 2 hours where the conditions are optimal for adsorption at 37°C. To terminate the adsorption process, the flask was taken out and 3ml of virus growth medium was added to the flask. The virus growth medium is made out of EMEM (ATCC 30-2003) and 2% FBS (ATCC 30-2020). In a 500ml bottle of EMEM, 10ml of FBS were added. 5ml of Pen-Strep solution was also added to a concentration of 1%. The flask was then placed back in the CO<sub>2</sub> incubator for a total of 12 days. The cells were monitored after 6 days to ensure proper inoculation of the cells. Before harvesting the virus, the culture flask containing SV40 was placed under a light microscope and the viral particles were counted to find their approximate concentration. Pictures of a confluent cell layer and SV40 layer can be seen in figure 5 on the left.

The cytopathic effect (CPE) is the structural changes in the host cell that result from the viral infection of cells. It is caused by either the lysis of the host cells or the death of host cells due to the inability to reproduce [14]. The CPE can be visualized in figure 5. Once CPE is processed through about 80% of the monolayer, the content of the flask was collected and filtered through a 0.45 $\mu$ m surfactant-free cellulose acetate syringe filter obtained from Fisher Scientific (Titan3 syringe filter 17mm 0.45 $\mu$ m, 03050369). Two aliquots of 1ml were placed in sterile Eppendorf tubes and 2ml of growth medium was added to the sample to avoid an accelerated titer decrease due to small volume. The aliquots were stored at -80°C.

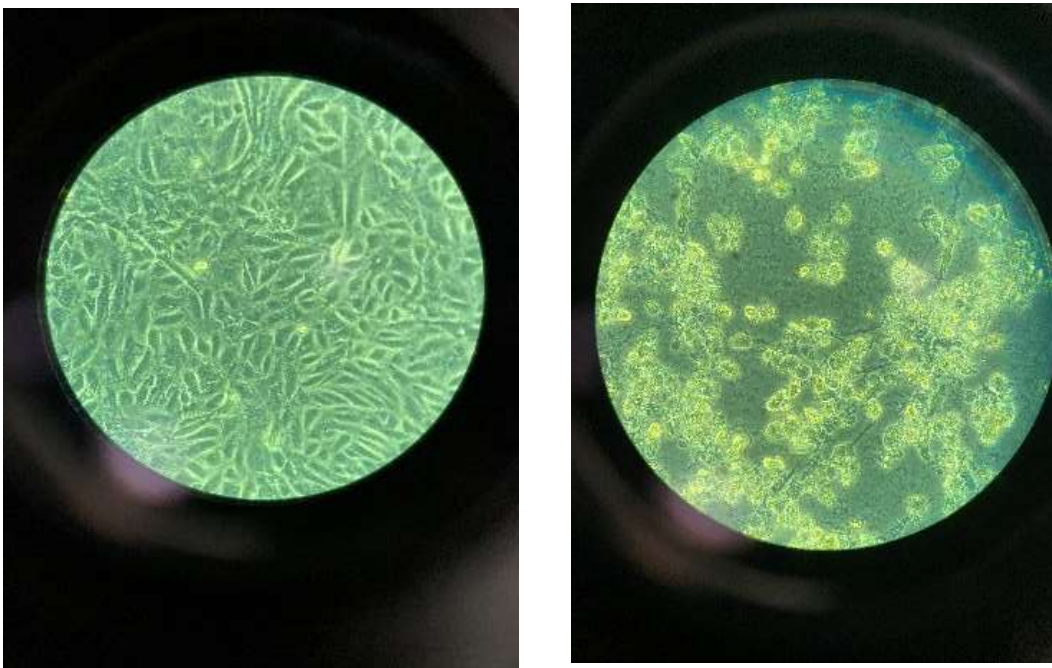


*Figure 5: Light microscope pictures of CV-1 cells (LEFT) and SV40 (RIGHT). These two pictures show the cytopathic effect. The cells on the right have been lysed and SV40 has reproduced.*

## 2.1 DETERMINATION OF PROTEIN CONCENTRATION

Antibodies were obtained from Abcam (Anti-SV40 VP1 ab53977) and (Anti-Adenovirus Type 5 antibodies ab6982). Upon reception, the solutions were each split into two aliquots. 2 $\mu$ l were placed on a Take3 plate. The Take3 program of the plate reader (Biotek Synergy H1 (Winooski, Vermont)) was used in pair with the Gen5 software to determine protein concentration of the antibodies and Type 5 hexon protein. Sterile ultrapure water was used as a reference for the program. The Beer-Lambert law was used to determine the protein concentrations of the analytes [15]. The Beer-Lambert law is written as such:

$$A = \epsilon l C$$

Where A is the absorbance,  $\epsilon$  is the protein extinction coefficient (mg/ml)<sup>-1</sup>cm<sup>-1</sup>, l is the pathlength (cm), and C is the protein concentration (M). The path length of the plate reader is 0.05cm. The calculation of the protein concentration of the antibodies and antigen from their absorbance is required to get a general idea of how much biotin to add later on. Therefore, we can estimate the protein extinction coefficient to be 1(mg/ml)<sup>-1</sup>cm<sup>-1</sup> for all analytes. Rearranging the Beer-Lambert equation to get the concentration, we get

$$C = \frac{A}{l\epsilon}$$

The absorbencies and concentrations were computed and are displayed in Table 1.

Analyte	Absorbance	Concentration (mg/ml)
Ab VP1	0.047	0.94
Ab Type 5	0.048	0.96
Hexon Protein Type 5	0.044	0.88

*Table 1: Absorbance and calculated protein concentration for each of the antibodies and antigen used.*

## **2.2 PREPARATION OF MICROSPHERES**

Streptavidin coated dyed polystyrene microspheres with nominal diameter of 0.19  $\mu\text{m}$  (Bangs Laboratories, CP01001) were obtained. In order to remove stabilizers and antimicrobial agents used by the manufacturer, the microspheres were washed four times in 0.1M PBS. Vivaspin Spin-X concentrator columns (Spin-X UF-500 Concentrator 500uL, 100,000 MWCO, 431481) were used to wash the microspheres.

## **2.3 BIOTINYLATED SP1 AND TYPE 5 ANTIBODIES**

Biotin (Thermo Scientific EZ-Link Sulfo-NHS-Biotin) was prepared separately following the Thermo Fisher protocol for biotinylating proteins [16]. Biotin was taken out of the freezer and allowed to reach room temperature before being used. Thermo Fisher provides a calculation sheet based on experiments ran with different protein and reagent concentrations. According to these experimental calculations, when a 20-fold excess of biotin was added to a 1-10 mg/ml antibody solution, the results were that 4 to 6 biotin groups bound to each antibody molecule. This concentration of biotin reagent on antibodies suits the desired amount to assemble to microsphere complexes. Thus, because of the concentration of SP1 antibody is 0.94 mg/ml and the concentration of the Type 5 antibodies is 0.96 mg/ml, a 20 fold excess meant that it was necessary to add 20mg/ml of the biotin reagent to each solution. The PDF used for calculations is added as a reference [17]. Subsequently, the antibodies were resuspended in sterile deionized water at a concentration of 20 fold excess to the biotin concentration. Biotin and antibodies were combined and incubated on ice for two hours. Once the incubation period ended, 2kD molecular weight cut off dialysis cassettes (Slide-A-Lyzer, Thermo Scientific) was used to remove the excess biotin from the reagents.



## **2.4 BIOTINYLATED TYPE 5 HEXON PROTEIN**

The Type 5 hexon proteins were biotinylated using the same method as the antibodies. Because both are proteins, the same procedure applies. The concentration of antigen was 0.88 mg/ml. Thus, a 20-fold excess results in the addition of 20 mg/ml of the biotin reagent to the solution as well. The antigens were resuspended in sterile deionized water with a concentration of 20 fold excess to the biotin concentration. Type 5 hexon protein and biotin were combined and incubated on ice for two hours, Once the incubation period ended, 2kD molecular weight cut off dialysis cassettes (Slide-A-Lyzer, Thermo Scientific) was used to remove the excess biotin from the reagents.

## **2.5 ATTACHING BIOTINYLATED ANTIBODIES TO PREPARED MICROSPHERES**

Freshly biotinylated SP1 and Type 5 antibodies were incubated with the washed streptavidin-coated microspheres at room temperature in the biohood for 30 minutes. Same concentrations of both antibodies were added to the sample to allow for even dispersion on the surface of the microspheres. The solution was mixed gently throughout the incubation period to allow for a uniform bonding between the microspheres and the antibodies. Once the incubation period was over, the antibody-covered microspheres were washed ten times in sterile deionized water to remove any unbound biotinylated antibodies from the solution. The concentration of the microspheres with bound antibodies was done using slow speed centrifugation. The antibody-coated beads were resuspended in 0.1M PBS at a pH of 7.4 to optimal storage concentration (0.5 mg-ml). The antibody-covered microspheres were stored at -20°C in an Eppendorf tube. This process was repeated to achieve the attachment of biotinylated Type 5 hexon proteins to microspheres. This process can be visualized in figure 6.

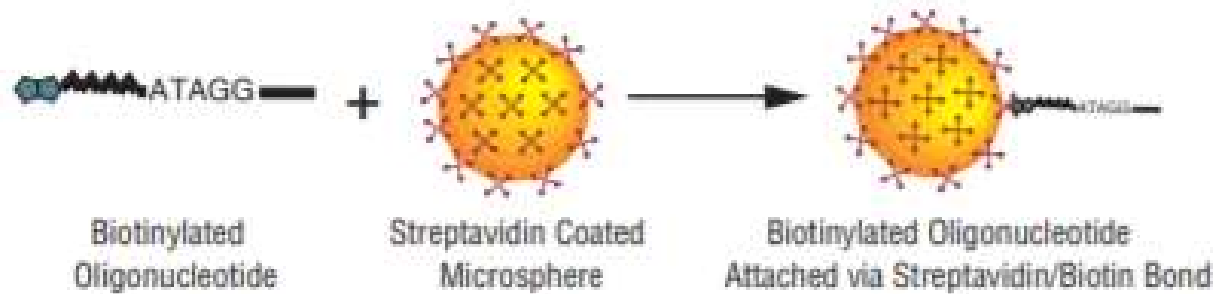


*Figure 6: Illustration of the process of attaching biotinylated antibodies to microspheres from Bangs Laboratories. The illustrated oligonucleotide represents the antibody or antigen used in this procedure.*

## 2.6 LABELLING SV40

The aliquot of SV40 that was used for this step was thawed at 4°C for 12 hours before using. A tenfold excess of antibody-covered microspheres was added to the virus. The virus and the microspheres were incubated at 24°C for 30 minutes under gentle agitation to allow the VP1 antibodies to bind to the attachment sites of the viral particles. Once the microspheres were bound to the viral particles, the solution was filtered using a 0.2µm surfactant-free cellulose acetate syringe filter (Fisher Scientific, 42213-CA). The microsphere complexes were eluted from the filter using sterile deionized water. The unbound microspheres are slightly smaller than the pore diameter of the filter, allowing for the sample to be mostly free of unbound microspheres.

## 2.7 FORMATION OF MICROSPHERE COMPLEXES

Sterile deionized water was run through the photoacoustic glow cytometry system to demonstrate the control background detection signal. 0.1 ml of sample containing only untagged

SV40 was run through the system. No detections were observed for unbound SV40 showing the absence of photo absorbers on its surface producing no photoacoustic response at 2mJ energy. The purified sample of MC1's was diluted to a total volume of 250 $\mu$ l and tittered through the photoacoustic flow cytometry system. No microsphere complexes were detected by the system. Next, the second layer of microspheres was bound to the microsphere complexes. Microspheres covered in native Adenovirus Type 5 hexon protein were titrated in the sample of MC1's and the solution was incubated at room temperature for 30 minutes. The mixture was gently mixed during the incubation period to allow for uniform attachment of the anti-adenovirus-antibody-covered microspheres over the surface of the MC1's. The unbound microspheres were removed from the sample again using a 0.2 $\mu$ m surfactant-free cellulose acetate syringe filter (Fisher Scientific, 42213-CA). The newly formed second microsphere complexes were eluted from the filter using sterile deionized water. This step yields a solution containing the double-layered microsphere complexes MC2. The aliquot containing the newly formed MC2's is tittered through the photoacoustic flow cytometry system. The second microsphere complexes yield a significant number of detections leading to the conclusion that covering single viral particles with tagged microspheres allows for the detection of viral analytes in solution using PAFC.

## **CHAPTER 3: RESULTS**

### **3.1 NEGATIVE CONTROLS**

Deionized ultrapure water was run through the photoacoustic flow cytometry system to assess the background noise level. Next, a sample containing solely viral particles was tittered through the system. The solution of viral particles was tittered to a concentration of about 4000 virions per ml. Thus the expected number of detections is about 1000 virions per test. No

detections were observed for virions alone or deionized ultrapure water, demonstrating their lack of photo absorbing ability resulting in no production of a photoacoustic response using 2mJ energy. CV-1 cells were also tittered through the system to make sure no remnant of the infected cells could result in detections. CV-1 cells alone did not trigger a detection from the system. Next, microspheres covered in SP1 and Type 5 antibodies were ran through the system. These were still too small to reach the detection threshold of the system and get detected. SV40 and the second layer of microspheres covered in Type 5 hexon proteins were combined in solution and tittered through the system. No detection resulted from mixing the two incompatible analytes. When the first microsphere complexes were analyzed in the system, one single detection was observed in two of the three rounds of experiments. Table 2 illustrates the results obtained from the negative control experiments.

Analyte	Detections Run 1	Detections Run 2	Detections Run 3
Ultrapure Water	0	0	0
SV40	0	0	0
VP1 Antibody + Type 5 Antibody Microspheres	0	0	0
Type 5 hexon protein Microspheres	0	0	0
CV-1 Cells	0	0	0
MC1	0	2	0
SV40 + Type 5 hexon protein Microspheres	0	0	0

*Table 2: Negative controls showing that no analyte contained in the microsphere complexes contain photo absorbing matter.*

### 3.2 POSITIVE CONTROLS

As a test of positive controls, we first tested 1 $\mu$ m polystyrene black microspheres. We added 4000 microspheres per milliliter. Each test was 250ul averaging 1000 microspheres per test. We obtained constant detections demonstrating that our system is working properly and

detects 1 $\mu$ m microspheres. Next, unmodified 0.19 $\mu$ m black microspheres were titrated in. No detections were obtained until microspheres reached a  $1 \times 10^8$  microspheres/ml concentration. Table 3 illustrates the results obtained from the positive control experiments. As an additional control, VP1 antibody tethered microspheres and Type 5 antibody tethered microspheres were combined leading to the hypothesis that this would result in unrestricted binding causing all the microspheres to form a large mass. The binding of these microspheres was visually observed and caused a clog in the PAFC system and had to be mechanically resolved.

<b>Concentration (Microspheres/ml)</b>	<b>0.19<math>\mu</math>m Microspheres</b>	<b>1<math>\mu</math>m Microspheres</b>
1x10 <sup>5</sup>	0	513
1x10 <sup>6</sup>	0	962
1x10 <sup>7</sup>	0	>990
1x10 <sup>8</sup>	4	>990
1x10 <sup>9</sup>	2	>990
1x10 <sup>10</sup>	752	>990

*Table 3: Positive controls showing that 0.19 $\mu$ m microspheres cannot absorb laser light until present in a concentration of  $10^8$  microspheres/ml. 1 $\mu$ m microspheres absorb laser light much better and can be detected starting from a  $10^5$  microspheres/ml concentration.*

### 3.3 EXPERIMENTAL DATA

The experimental data is represented as ratios of analytes combined. The relative number of viral particles is always 1 because we want to show that a single viral particle can be detected by adding an appropriate number of microspheres. The data obtained from the ratio experiments are shown in table 4. The assumption that six binding sites exist on the surface of each viral particle justify the relative number of 6 antibody-covered microspheres added to the sample. By saturating the surface of the viral particles with microspheres, we are assured that they will be covered by the second layer of microspheres in the next step. Keeping a relatively low number of antibody-covered microspheres also gives us insurance that the antigen-covered microspheres

will bind to the complexes until saturation. The excess of antigen-bound microspheres will remain free-floating in the sample and can be discarded. The data obtained from adding a ratio of 1000 Type 5 antigen microspheres is only slightly higher than the data obtained from adding a ratio of 100 Type 5 antigen microspheres. Because the difference remains below one order of magnitude, it is not justified to add ten times more Type 5 microspheres to the solution. The same results are to be expected and less resources are needed. Table 5 illustrates the summarized data leading to the conclusion that single viral particles can be detected by the PAFC system using appropriately tagged microspheres.

<b>Ratio (SV40: VP1/Type 5 Microspheres: Type 5 antigen Microspheres)</b>	<b>Detections Run 1</b>	<b>Detections Run 2</b>	<b>Detections Run 3</b>
1:1:1	0	0	0
1:6:1	0	0	0
1:6:100	587	565	489
1:6:1000	603	611	599

*Table 4: Experimental data showing that ratios of SV40 to VP1 antibody Microspheres to Type 5 hexon protein microspheres. Increasing the amount of Type 5 hexon protein microspheres does not alter the outcome much because the surface area of the first microsphere.*

<b>Analyte</b>	<b>Detections Run 1</b>	<b>Detections Run 2</b>	<b>Detections Run 3</b>
SV40 alone	0	0	0
MC1	1	1	0
MC2 (1:6:100)	587	565	489

*Table 5: Summary of the experimental data. The number of detections obtained from the second Microsphere Complexes is two orders of magnitude higher than that of the first Microsphere Complexes.*

## CHAPTER 4: DISCUSSION

This study demonstrates the ability of PAFC to be used for single viral particle detection *in vitro*. Additionally, the method created uses a double layer of microspheres which represents an advancement in specificity. This method complements the current demonstrated abilities of the PAFC system and could be patented in the future.

No difference was observed between background noises observed from ultrapure water and the viral sample. The data shows that 1 $\mu$ m black microspheres yield detections starting at much lower concentrations than 0.19 $\mu$ m black microspheres. 0.19 $\mu$ m black microspheres do not yield detections unless they are present in very high concentration in the sample. At  $1 \times 10^{10}$  microspheres/ml, we did obtain a significant detection level. Therefore, the presence of 19 $\mu$ m black microspheres in solution does not alter the data because they are only detected by the PAFC system when highly concentrated. Furthermore, we filtered out the unbound microspheres before eluting the microsphere complexes and processing them. It is unlikely that enough unbound microspheres are found in the sample that we obtain a false positive detection. The experimental data shows a clear correlation between the formation of MC2's and detections of particles. After adding the first layer of microspheres on the viral particles and forming MC1's, no detections were obtained. Also, adding the second layer of microspheres in a ratio of 1:6:1 also does not yield detections. After adding Type 5 antigen-bound microspheres in a ratio of 1:6:100, we get a significant number of detections from the PAFC system. The pressure wave resulting from the thermoelastic reaction within MC2's in a ratio of 1:6:100 is greater than the detection threshold of the transducer. The data shows that adding Type 5 antigen-tittered microspheres to the sample in a ratio of 1:6:1000 does not result in a drastic change of the number of detections obtained. Thus, is it not justified to add Type 5 antigen-bound

microspheres to the sample in a ratio superior to 1:6:100. Table 5 aids the visualization of the results obtained from the three main steps of this study. Viral particles alone do not contain photo-absorbing matter and therefore cannot be detected by the PAFC system. As for the MC1's, we obtained one detection per run of 250 $\mu$ l sample. These complexes were made by adding a concentration of 40 000 microspheres/ml to a 4000 viral particles/ml sample (1:10 viral particles to microspheres ratio). Therefore, if MC1's could be detectable by the PAFC system, we would expect to see close to 1000 detections for the 250 $\mu$ l sample. However, we only obtained one detection twice over three runs. Free-floating unbound MC1's thus do not alter the MC2 detection data. The single detections can be attributed to undesired analytes present in the sample or static charge build up caused by the polystyrene beads [18]. This is an area that can be improved in the future to avoid false positive detections. The MC2's detection data shows that the noise resulting from the thermoelastic reaction within them can be detected by the PAFC system. The initial number of viral particles added to the sample was about 1000 virions/test. Due to the size of the added antibody-coated microspheres, it is possible that not all virions became coated with microspheres, eliminating some viral particles from the sample. The numbers of detections of MC2's for each run is still more than half the initial number of viral particles present in the sample. Also, it is two orders of magnitude higher than that of the viral particles alone or MC1's. Thus, we can affirm that the formation of a second microsphere complex resulting in layers of PAFC detectable microspheres results in the detection of single particle detection in sample. With this method of viral particle detection, the signal to noise ratio used to detect melanoma and bacterial cells can be maintained to detected viral particles, regardless of the size difference between the different analytes. This is an advantage, because it allows the system to become more versatile and increase its application range without wasting



time on energy-adjusting steps. The Photoacoustics procedure therefore remains the same and any trained individual can analyze a viral particle sample with the method. Another advantage of this method of viral detection is the time required to do the assay. A sample is prepared and ready to be processed within an hour. This is a big change from the other viral assay techniques currently used which are either not quantitative or require multiple days to yield results.

#### **4.1 FUTURE DIRECTIONS**

In the future, a way of increasing accuracy when using microsphere complexes with the PAFC system to detect viral particles is through signal detection threshold modulation. Finding the lower and higher bound of signal detection threshold for each complex will lead to the formation of a detection ladder. The most significant detection threshold will be the average threshold for the MC2's. Any signal above the higher bound can be discarded and categorized as an undesired analyte. Another way to better this system is if the laser energy is adjusted to maximize the level at which the microsphere complexes are detected. Some complexes with a lesser density or size might require a smaller amount of energy to get optimally detected. Some experimenting will be helpful to determine the optimal nominal diameter of the microsphere for different size ranges of viral particles. Additionally, the color of the chosen microspheres for each layer can be chosen to be different in order to make the detection of a specific layer possible. Specific wavelengths have a specific absorption spectrum. For this reason, pairing the microsphere color to the laser wavelength brings an additional level of specificity to the method. This addition could decrease the time needed for various types of particle detection. The difficulty linked to the combination of two antibody-antigen pairs when constituting MC2 is that the second pair needs to correspond to a virus that is not of interest. This is a necessary

component of the assembly of the microsphere complex to avoid free-floating microspheres that have attached to viral particles but that are not part of a microsphere complex. Consequently, an “antibody cocktail” could be engineered to yield the most time-efficient detection of the analytes. Statistical analysis would need to be performed and take into consideration multiple families of viruses to yield the best combination needed to optimize targeted viral detection. Moreover, this technique could be used to detect multiple analytes in a same sample. By using different colored microspheres and being able to change the laser wavelength, one sample containing multiple targeted particles can be analyzed in a fraction of the time needed to analyze multiple samples.

## **4.2 CONCLUSION**

Timely and accurate detection of viral contaminants is important to control known or unknown viral outbreaks. RT PCR has been the gold standard for viral particle identification because of its ability to qualitatively identify the infectious particle. However, this method takes at least 8 hours to carry on and is not quantitative. There exists a need for more rapid viral diagnostics systems that can identify and quantify the contaminants to aid medical professional administer the most relevant care to patients. The photoacoustic flow system paired with tagged microspheres has the ability to not only qualitatively discriminate the viral particle in question, but also to give a quantitative assay of the number of virions in a sample. This simple yet innovative method of viral particle detection can also be expanded upon through signal detection threshold modulation or by using microspheres with different absorbance spectra. This method can be used in the future and refined to contribute to the timely need for relevant contributions against viral outbreaks.

## REFERENCES

1. Sanjuán, R., *Collective properties of viral infectivity*. Current Opinion in Virology, 2018. **33**: p. 1-6.
2. Reta, D.H., et al., *Molecular and Immunological Diagnostic Techniques of Medical Viruses*. International Journal of Microbiology, 2020. **2020**: p. 8832728.
3. Nasrollahi, F., et al., *Micro and Nanoscale Technologies for Diagnosis of Viral Infections*. Small. **n/a(n/a)**: p. 2100692.
4. Paltauf, G., H. Schmidt-Kloiber, and M. Frenz, *Photoacoustic waves excited in liquids by fiber-transmitted laser pulses*. The Journal of the Acoustical Society of America, 1998. **104(2)**: p. 890-897.
5. Galanzha, E.I., et al., *In vivo magnetic enrichment and multiplex photoacoustic detection of circulating tumour cells*. Nature Nanotechnology, 2009. **4(12)**: p. 855-860.
6. Edgar, R., et al., *Bacteriophage-mediated identification of bacteria using photoacoustic flow cytometry*. Journal of Biomedical Optics, 2019. **24(11)**: p. 115003.
7. O'Brien, C., et al., *Capture of circulating tumor cells using photoacoustic flowmetry and two phase flow*. Journal of Biomedical Optics, 2012. **17(6)**: p. 061221.
8. Brenner, A.V., et al., *Polio Vaccination and Risk of Brain Tumors in Adults*. No Apparent Association, 2003. **12(2)**: p. 177-178.
9. Liddington, R.C., et al., *Structure of simian virus 40 at 3.8-Å resolution*. Nature, 1991. **354(6351)**: p. 278-84.
10. Johnson, J.E. and A.J. Olson, *Icosahedral virus structures and the protein data bank*. J Biol Chem, 2021. **296**: p. 100554.

11. Kawano, M., et al., *SV40 VP1 major capsid protein in its self-assembled form allows VP1 pentamers to coat various types of artificial beads in vitro regardless of their sizes and shapes*. Biotechnology reports (Amsterdam, Netherlands), 2014. **5**: p. 105-111.
12. Martinez-Hernandez, F., et al., *Single-virus genomics reveals hidden cosmopolitan and abundant viruses*. Nature Communications, 2017. **8**(1): p. 15892.
13. Allen, L.Z., et al., *Single virus genomics: a new tool for virus discovery*. PLoS One, 2011. **6**(3): p. e17722.
14. Agol, V.I., *Cytopathic effects: virus-modulated manifestations of innate immunity?* Trends in Microbiology, 2012. **20**(12): p. 570-576.
15. Pace, C.N., et al., *How to measure and predict the molar absorption coefficient of a protein*. Protein science : a publication of the Protein Society, 1995. **4**(11): p. 2411-2423.
16. ThermoFisher, *Avidin-Biotin Handbook*.
17. BangsLaboratories. *Working with Microspheres*. 2013.
18. Burgo, T.A.L., et al., *Friction coefficient dependence on electrostatic tribocharging*. Scientific reports, 2013. **3**: p. 2384-2384.